A Mathematical Model Exploring the Impact of Climatic Factors on Malaria Transmission Dynamics in Burundi

Gatore Sinigirira, Kelly Joëlle; Et al.

2024-11
Journal of Applied Mathematics and Physics
https://repository.ub.edu.bi/handle/123456789/2154
Gatore Sinigirira, K.J., Ogana, W., Nyandwi, S., Kwizera, J.D.D. and Niyukuri, D. (2024) A Mathematical Model Exploring the Impact of Climatic Factors on Malaria Transmission Dynamics in Burundi. Journal of Applied Mathematics and Physics, 12, 3728-3757.
https://doi.org/10.4236/jamp.2024.1211224

Journal of Applied Mathematics and Physics, 2024, 12, 3728-3757
https://www.scirp.org/journal/jamp
ISSN Online: 2327-4379
ISSN Print: 2327-4352

A Mathematical Model Exploring the Impact of Climatic Factors on Malaria Transmission Dynamics in Burundi

Kelly Joëlle Gatore Sinigirira[1,2], Wandera Ogana[3,4], Servat Nyandwi[2], Jean De Dieu Kwizera[5,6], David Niyukuri[1,2,7]

[1]Doctoral School, University of Burundi, Bujumbura, Burundi
[2]Department of Mathematics, University of Burundi, Bujumbura, Burundi
[3]Department of Mathematics, University of Nairobi, Nairobi, Kenya
[4]African Mathematics Millennium Science Initiative (AMMSI), Nairobi, Kenya
[5]Faculté de Sciences, Institut Supérieur des Cadres Militaires (ISCAM), Bujumbura, Burundi
[6]Department of Public Health, Mount Kenya University, Thika, Kenya
[7]The South African Department of Science and Technology-National Research Foundation (DST-NRF) Centre of Excellence in Epidemiological Modelling and Analysis (SACEMA), Stellenbosch University, Cape Town, South Africa
Email: kelly.gatore@ub.edu.bi, wogana@uonbi.ac.ke, servat.nyandwi@ub.edu.bi, kwizera136@gmail.com, david.niyukuri@ub.edu.bi

How to cite this paper: Gatore Sinigirira, K.J., Ogana, W., Nyandwi, S., Kwizera, J.D.D. and Niyukuri, D. (2024) A Mathematical Model Exploring the Impact of Climatic Factors on Malaria Transmission Dynamics in Burundi. *Journal of Applied Mathematics and Physics*, **12**, 3728-3757.
https://doi.org/10.4236/jamp.2024.1211224

Received: July 23, 2024
Accepted: November 12, 2024
Published: November 15, 2024

Abstract

Mathematical modeling plays a crucial role in understanding the dynamics of malaria transmission and can provide valuable insights for designing effective control strategies. Malaria indeed faces significant challenges due to a changing climate, particularly in regions where the disease is endemic. This disease is significantly impacted by changes in climate, especially rising temperatures and fluctuating rainfall patterns. This study explores the influence of temperature and rainfall abundance on malaria transmission dynamics within the context of Burundi. We have constructed a deterministic model that integrates these climatic parameters into the dynamics of the human host-mosquito vector system. The model's steady states and basic reproduction number, calculated using the next-generation method, reveal important insights. Numerical simulations demonstrate that both temperature and rainfall significantly influence mosquito population dynamics, leading to distinct effects on malaria transmission. Specifically, we observe that temperatures between 20˚C and 32˚C, along with rainfall ranging from 10 to 30 mm per month, create optimal conditions for mosquito development, thus driving malaria transmission in Burundi. Furthermore, our findings indicate a delayed relationship between rainfall and malaria cases. When rainfall peaks in a given month, malaria does not peak immediately but instead shows a lagged response. Similarly, when

rainfall decreases, malaria incidence drops after a certain time lag. This same lagged effect is observed when comparing temperature with confirmed malaria cases in Burundi. These findings highlight the urgent need to consider climate factors in malaria control strategies.

Keywords

Malaria, Temperature, Rainfall, Reproduction Number and Analysis

1. Introduction

Malaria is a disease transmitted by Plasmodium protozoan parasites and spread through the bite of female Anopheles mosquitoes [1]. It stands as a substantial public health concern worldwide, with particular gravity evident in Burundi [2]. The infectious disease is responsible for millions of cases annually, with a substantial percentage occurring in sub-Saharan Africa [3]. During a blood meal, female anopheles mosquitoes collect plasmodium parasites on an infectious person. After their development, the parasites migrate to the salivary gland and can be transmitted to susceptible human hosts during another blood meal [4] [5]. The impact of climate change on human health is becoming a more significant issue, with noticeable effects seen in various infectious diseases, such as the transmission of malaria [6]. Rapid environmental fluctuations, such as changes in temperature and rainfall, pose challenges to existing control and eradication strategies. Hence, recognizing the significance of temperature and rainfall in the transmission of malaria becomes particularly crucial.

Temperature plays a critical role in the life cycle of the malaria vector, exerting a significant influence on the development of its aquatic stages and their transition to adulthood. The hatching duration of mosquito eggs varies with temperature, with incubation periods of 1, 3, and 10 days observed at 30˚C, 20˚C, and 10˚C, respectively. Furthermore, water temperature serves as a regulatory factor in the pace of mosquito breeding [7]. In 2019, malaria ranked as the fourth leading cause of death in Burundi, following diarrhea, neonatal disorders, and tuberculosis [8]. The country has witnessed a troubling surge in malaria cases, increasing from 2.6 million in 2013 to 8.3 million in 2016 [9]. Approximately four-fifths of the population in Burundi is at risk, with less than two-thirds living in potentially epidemic areas and the other third in hyper-endemic regions. Malaria-related outpatient consultations account for half of health facility visits, and pregnant women and children under 5 years old are the most vulnerable groups, comprising 48% of deaths in this age range [10].

The rise in malaria transmission is attributed to factors such as low usage of preventive measures, decreased population immunity, especially in mountainous areas with traditionally low malaria transmission, and changes in climate affecting vector ecology and behavior [10]. Climate change is expected to exacerbate malaria transmission in Africa, with rising temperatures projected to surpass 2˚C by

2100 [9]. Regions that were once considered less prone to malaria due to their cooler climates are now facing increased invasion by the disease. Malaria is highly sensitive to climatic conditions, thriving in tropical climates due to favorable breeding sites and temperatures [11]. Small changes in temperature can significantly impact mosquito lifespan, explaining the prevalence of the disease in tropical regions [12]. The proliferation of mosquitoes is closely tied to climatic conditions and the availability of oviposition sites, influenced by natural and environmental factors [13]. Changes in temperature, humidity, precipitation, and wind speed impact malaria incidence by altering the life cycles of mosquitoes and parasites or influencing the behavior of humans, vectors, and parasites [14] [15]. Higher temperatures accelerate mosquito digestion, leading to more frequent human bites and increased disease transmission [16].

Malaria transmission models play a crucial role in decoding and interpreting the dynamics of the disease and directing possible intervention strategies [17]. Early models, such as Ross's susceptible-infective-susceptible (SIS) model, laid the foundation for understanding the link between mosquito populations and human malaria incidence [18]. The author found that malaria can not persist when the number of mosquitoes is below a certain threshold. However, subsequent improvements by various authors emphasized the importance of mosquito lifespan in malaria transmission. Models incorporating acquired immunity to malaria based on exposure have also been explored [19]-[22]. Macdonald showed that lowering the number of mosquitoes will not reduce malaria disease, but the lifespan of mosquitoes is the most important factor in the transmission of malaria [22].

The relationship between malaria and climate factors in East Africa is significant [16]. Numerous studies underscore the role of environmental and climatic factors in the dynamic transmission of malaria [6] [23] [24]. Research indicates that the transmission of malaria in East Africa is closely linked to climate elements, particularly temperature and rainfall, highlighting the complex connection between climate change and the prevalence of malaria in the region [25] [26]. Burundi is an African country located in East Africa, situated between latitudes 2.3 S and 4.5 S and longitudes 29 E and 31 E. Despite the country's relatively small size (27,834 km^2), the distribution of its diverse topography accurately represents the variations in its climate. As a result, precipitation is unevenly distributed across the country. Recent work on malaria transmission dynamics in Burundi highlights the critical role of temperature and mosquito behavior in disease spread. Sakubu *et al.* employed deep learning models to predict malaria cases in Burundi, integrating climate variables such as temperature, rainfall, and humidity. Their predictive analysis demonstrated that climatic factors have a significant impact on malaria dynamics, offering precise forecasts at both provincial and national levels [27]. In [28], the authors developed a deterministic SEIR model. Their findings underscored that the number of mosquito bites, which is strongly influenced by temperature, along with the vector population, are critical factors in reducing

malaria spread. In Burundi, the temperature is generally warm, ranging from 15˚C to 35˚C. These conditions provide favorable environments for mosquito breeding. Hence, it can lead to increased mosquito populations and heightened transmission of malaria, exacerbating the prevalence and spread of the disease. The distribution of temperature and rainfall within Burundi is shown in **Appendices B** and **C**, respectively.

Transmission of malaria disease occurs consistently throughout the year, but there are two specific times when transmission peaks. These peak periods typically happen from March to June and from October to December. When analyzing the monthly number of cases over the 8-year period in **Appendix A**, it becomes apparent that despite variations in magnitudes and disparities within individuals, the overall trend across the months resembles. Specifically, there is a consistent pattern where the number of infections is high in January, decreases in February, and starts increasing from April to June, followed by a sharp decline during the summer months, reaching the lowest cases in August. Subsequently, there has been a resurgence in cases since September, peaking in December.

This research paper investigates the relationship between climate variables, specifically temperature and rainfall, and the occurrence of malaria through the use of a malaria transmission mathematical model. The study aims to address the fundamental question of how these climate factors affect the prevalence of malaria. We employ a dynamic model that considers the influence of climate conditions on mosquitoes. Importantly, we utilize real data to determine the values of the model parameters. This method is crucial for conducting computer simulations of dynamic processes, ensuring accurate estimations of parameters and predictions for how the system will respond.

Section 2 provides a detailed description of the model. In that section, we show the domain in which the model remains epidemiologically well-posed. Furthermore, we discuss the existence of equilibria, including the calculation of the fundamental reproduction number and an examination of the equilibria's stability. Numerical simulation contains numerical simulations of the model and observations. We finish by discussing the results in Section 4.

2. Model Formulation

In this model, we formulate a mathematical model that takes into account the effects of climate factors on malaria transmission dynamics by emphasizing the impact of temperature and rainfall in the model. The disease is modeled using ordinary differential equations (ODEs) where humans and mosquitoes infect each other.

The total population is divided into four classes, namely: susceptible class $S_h(t)$, those who are exposed to malaria parasites $E_h(t)$ but not infectious, individuals with malaria symptoms $I_h(t)$ and the class of recovered individuals $R_h(t)$. This is known as the SEIR compartmental model.

We assume that immunity is temporary, which means that individuals who are

recovered from the disease have immunity against the malaria parasite for a certain period. Susceptible individuals are recruited into the population at a rate α_h and acquire malaria through a bite of an infectious mosquito and progress to the exposed class $E_h(t)$ through a force of infection λ_h. Exposed individuals move then to the infectious class at rate ρ_h. Infected humans recover at rate γ_h and die at rate δ due to malaria infection, and recovered individuals lose their immunity at a rate q. Susceptible, exposed, and recovered humans die at the same natural death rate, but in addition to this rate, infected humans die due to malaria parasites. Mosquito populations are recruited at a per capita rate $\theta_v(T,R)(1-N_v/K)$ where $\theta_v(T,R)$ is the birth rate of mosquitoes. The birth rate of mosquitoes is affected by climate conditions. In particular, temperature and rainfall have the potential to both decrease and increase it. This indicates that temperature and rainfall have a complex relationship with mosquito population growth [29]. Let K be the environmental carrying capacity of the pupa. Mosquitoes die at a per capita natural death rate $\mu_v(T)$, we assume that the mosquito doesn't face extinction by defining $\alpha_v = \theta_v - \mu_v > 0$. After a bite on an infected human, susceptible mosquitoes will then become exposed and progress to the class of infected mosquitoes $I_v(t)$. Infected mosquitoes remain infected all their life. We assume that all newborns are susceptible to the disease in the human host and vector populations. The flow diagram presented in **Figure 1** shows how mosquitoes and human hosts interact dynamically, highlighting the changes across various classes. It represents the process through which individuals can move from one class to another within the system, capturing the complexity of interactions between humans and mosquitoes.

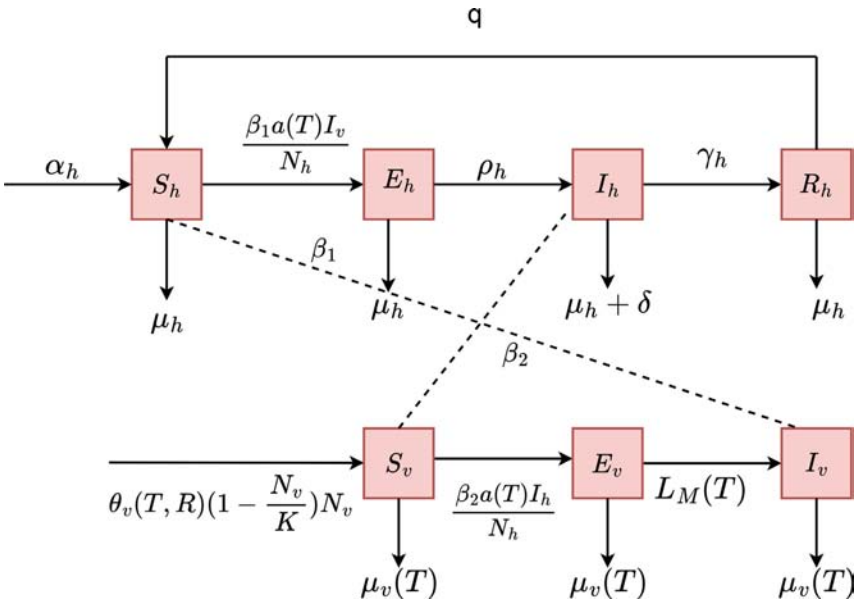

Figure 1. Flow diagram for the transmission dynamics of malaria.

The dynamic transmission of malaria between humans and mosquitoes is described by the following system of non-linear ordinary differential equations.

$$\begin{cases} \dfrac{\mathrm{d}S_h}{\mathrm{d}t} = \alpha_h + qR_h - \dfrac{\beta_1 a(T) I_v(t)}{N_h} S_h - \mu_h S_h, \\ \dfrac{\mathrm{d}E_h}{\mathrm{d}t} = \dfrac{\beta_1 a(T) I_v(t)}{N_h} S_h - (\rho_h + \mu_h) E_h, \\ \dfrac{\mathrm{d}I_h}{\mathrm{d}t} = \rho_h E_h - (\mu_h + \gamma_h + \delta) I_h, \\ \dfrac{\mathrm{d}R_h}{\mathrm{d}t} = \gamma_h I_h - (\mu_h + q) R_h, \\ \dfrac{\mathrm{d}S_v}{\mathrm{d}t} = \theta_v(T,R)\left(1 - \dfrac{N_v}{K}\right) N_v - \mu_v(T) S_v - \dfrac{\beta_2 a(T) I_h(t)}{N_h} S_v, \\ \dfrac{\mathrm{d}E_v}{\mathrm{d}t} = \dfrac{\beta_2 a(T) I_h(t)}{N_h} S_v - \mu_v(T) E_v - L_v(T) E_v, \\ \dfrac{\mathrm{d}I_v}{\mathrm{d}t} = L_v(T) E_v - \mu_v(T) I_v, \end{cases} \tag{1}$$

with the following initial conditions $S_h(0) = S_h^0 > 0$, $E_h(0) = E_h^0 \geq 0$, $I_h(0) = I_h^0 \geq 0$, $R_h(0) = R_h^0 \geq 0$, $S_v(0) = S_v^0 > 0$, $E_v(0) = E_v^0 \geq 0$, $I_v(0) = I_v^0 \geq 0$.

Table 1. Variables of the basic malaria model.

Variable	Definition	Unit
S_h	Susceptible Humans population	People
E_h	Exposed Humans Population	People
I_h	Infected Humans Population	People
R_h	Recovered Humans Population	People
S_v	Susceptible Mosquitoes Population	Mosquitoes
E_v	Exposed Mosquitoes Population	Mosquitoes
I_v	Infected Mosquitoes Population	Mosquitoes

The total human population is given by $N_h(t) = S_h(t) + E_h(t) + I_h(t) + R_h(t)$, whereas the total vector (mosquito) population is given by $N_v(t) = S_v(t) + E_v(t) + I_v(t)\ N_h(t)$.

Table 1 and Table 2 give the description of variables and parameters involved in the construction of the model.

Table 2. Variables and parameters of the basic malaria model.

Parameters	Definition	Unit
α_h	Recruitment rate of human populations	people/time
q	Progression rate of the human population from R_h to S_h	time^{-1}
β_1	Probability of transmission of malaria from an infectious vector to a susceptible human per contact	-

Continued

$a(T)$	Mosquito biting rate	bites/person*time
μ_h	Natural mortality rate of human population	time^{-1}
$\mu_v(T)$	Mortality rate of adult mosquitoes	time^{-1}
ρ_h	Progression rate of the human population from E_h to I_h	time^{-1}
γ_h	Progression rate of the human population from I_h to R_h	time^{-1}
δ	Disease-induced death rate	time^{-1}
$\theta_v(T,R)$	Recruitment rate of mosquitoes	time^{-1}
β_2	Probability of transmission of malaria from an infectious human to a susceptible vector per contact.	-
$L_v(T)$	Progression rate of mosquito population from E_v to I_v	time^{-1}
K	Carrying capacity of mosquitoes	mosquitoes

Section 3, modelanalysis, the parameter $\theta_v(T,R)$ will be simplified to θ_v, while $a(T)$ will be denoted as a. Similarly, $L_v(T)$ will be represented as L_v, and $\mu_v(T)$ will be expressed as μ_v. We also define the forces of infection

$$\lambda_h = \frac{\beta_1 a(T) I_v(t)}{N_h(t)} \text{ and } \lambda_v = \frac{\beta_2 a(T) I_h(t)}{N_h(t)},$$

which represent respectively in the model the rate at which susceptible humans become infected by infectious female anopheles mosquitoes and the rate at which susceptible mosquitoes become infected by infectious humans.

2.1. Model Properties

In this section, we show that our model is mathematically and biologically well-posed. To demonstrate it, we aim to prove that for all $t \geq 0$, the system of equations in (1) possesses positive solutions with positive initial conditions and remains bounded within a biologically meaningful and feasible positive region Ω. The region Ω should represent conditions that are biologically meaningful.

2.1.1. Positivity of Solutions

Theorem 2.1. *Given the initial conditions of the model* (1) *that are*, $S_h(0) = S_h^0 > 0$, $E_h(0) = E_h^0 \geq 0$, $I_h(0) = I_h^0 \geq 0$, $R_h(0) = R_h^0 \geq 0$, $S_v(0) = S_v^0 > 0$, $E_v(0) = E_v^0 \geq 0$, $I_v(0) = I_v^0 \geq 0$, *the solutions of the model remain positive for all* $t > 0$.

Proof. From the model (1), we have

$$\frac{dS_h}{dt}(t) = \alpha_h + qR_h(t) - \lambda_h S_h(t) - \mu_h S_h(t) \geq -(\lambda_h + \mu_h) S_h(t).$$

After integrating, we found that $S_h(t) \geq S_h^0 e^{-\left(\mu_h t + \int_0^t \lambda(s)ds\right)} > 0 \quad \forall t > 0$ as the exponential function is always positive and $S_h^0 > 0$, it ensures that the solution for $S_h(t)$ will stay positive for all time $t \geq 0$. We also have

$$\frac{dE_h}{dt}(t) \geq -(\rho_h + \mu_h) E_h(t),$$

which gives

$$E_h(t) \geq E_h^0 e^{-\left(\mu_h t + \int_0^t \rho_h(s)ds\right)} \geq 0 \quad \forall t > 0.$$

for

$$\frac{dS_v}{dt}(t) \geq -(\mu_v + \lambda_v) S_v(t),$$

we have

$$S_v(t) \geq S_v^0 e^{-\left(\mu_v t + \int_0^t \lambda_v(s)ds\right)} > 0 \quad \forall t > 0.$$

Using a similar approach, it can be demonstrated that the model's other state variables remain positive. □

2.1.2. Invariant Region

Lemma 2.2. *There exists a feasible region that is positively invariant, defined as* $\Omega = \Omega_H * \Omega_v$ *such that* $\Omega_H = \left\{(S_h, E_h, I_h, R_h) \in \mathbb{R}_+^4 : 0 \leq N_h \leq \frac{\alpha_h}{\mu_h}\right\}$, $\Omega_V = \left\{(S_v, E_v, I_v) \in \mathbb{R}_+^3 : 0 \leq N_v \leq \frac{K\alpha_v}{\theta_v}\right\}$, *which attracts all solutions with respect to the system* (1)

Proof. Adding the first four equations of the system (1) and the three remaining equations, we get

$$\begin{cases} \frac{dN_h}{dt} \leq \alpha_h - \mu_h N_h, \\ \frac{dN_v}{dt} \leq \frac{K\alpha_v}{\theta_v}. \end{cases} \tag{2}$$

Multiplying both sides of the first equation in the system (2) by $e^{\mu_h t}$ yields

$$e^{\mu_h t}\left(\frac{dN_h}{dt} + \mu_h N_h\right) \leq \alpha_h e^{\mu_h t},$$

$$\frac{d\left(N_h e^{\mu_h t}\right)}{dt} \leq \alpha_h e^{\mu_h t}. \tag{3}$$

Integrating both sides of system (3),

$$N_h(t) \leq \frac{\alpha_h}{\mu_h} + N_h(0) e^{-\mu_h t},$$

$$N_h(t) \leq \frac{\alpha_h}{\mu_h} + \left(N_h^0 - \frac{\alpha_h}{\mu_h}\right) e^{-\mu_h t}. \tag{4}$$

Using the theorem of differential inequality [30], we get

$$0 \le N_h(t) \le \frac{\alpha_h}{\mu_h}. \tag{5}$$

As $t \to \infty$, then

$$N_h(t) \le \frac{\alpha_h}{\mu_h}. \tag{6}$$

From the second equation of the system (2) given as

$$\frac{\mathrm{d}N_v}{\mathrm{d}t} = \alpha_v N_v - \frac{\theta_v N_v^2}{K},$$

we integrate the equation, we found that the total mosquito population is

$$N_v(t) = \frac{K\alpha_v N_v(0)}{\theta_v}.$$

$N_v(t)$ can not become 0 at any finite time. So, for $0 < N_v^0 \le \frac{K\alpha_v N_v(0)}{\theta_v}$, on $[0,\Omega)$ we have $0 < N_v(t) \le \frac{K\alpha_v}{\theta_v}$. Thus, Ω is bounded. For $t > 0$, every solution of the model (1) with positive initial conditions in Ω remains there.

2.2. Model Analysis

In this section of model analysis, we computed the disease-free equilibrium reproduction number, and we proved the existence of an endemic point. □

2.2.1. Disease-Free Equilibrium Point

The disease-free equilibrium point of the model represents a state where there are no infected individuals in the population, indicating a disease-free scenario. At this equilibrium, all compartments of the model that represent the disease have zero values, signifying that the disease is not present and transmission has ceased. Substituting $E_h = I_h = R_h = E_v = I_v = 0$ into equations of the model (1) and solving the resulting equations, we found that the disease-free equilibrium point of model (1) is described by:

$$E_0 = \left(\frac{\alpha_h}{\mu_h}, 0, 0, 0, \frac{K\alpha_v}{\theta_v}, 0, 0\right). \tag{7}$$

2.2.2. Reproduction Number

In epidemiological models, the fundamental reproductive number, known as R_0, represents the average number of secondary cases generated by a typical infected individual in a population that is entirely susceptible [31], this concept has been applied to evaluate R_0 in the context of diseases like malaria. When R_0 is less than 1, it indicates that, on average, the infected individual leads to fewer than one new infection during their period of contagiousness, ultimately causing the disease to decline. Conversely, if R_0 exceeds 1, it suggests that, on average, an infected individual results in more than one new infection within a fully susceptible community, indicating the persistence of the disease.

The basic reproduction number is calculated using the next-generation matrix theory. $R_0 = \rho\left(FV^{-1}\right)$, where $\rho\left(FV^{-1}\right)$ is the spectral radius of the matrix FV^{-1}. F and V are the matrices for new infection and transmission terms, respectively (see, for example, [32]).

Lemma 2.3. *The basic reproduction number of the system* (1) *is*

$$R_0 = \sqrt{\frac{\beta_1\beta_2 a^2(T)K\alpha_v\rho_h\mu_h L_v}{\theta_v\alpha_h\mu_v(\rho_h+\mu_h)(\mu_h+\delta+\gamma_h)(\mu_v+L_v)}} \tag{8}$$

Proof. We have:

$$f = \begin{pmatrix} \dfrac{\beta_1 a I_v S_h}{S_h+E_h+I_h+R_h} \\ 0 \\ \dfrac{\beta_2 a I_h S_v}{S_h+E_h+I_h+R_h} \\ 0 \end{pmatrix}; \quad v = \begin{pmatrix} (\rho_h+\mu_h)E_h \\ (\mu_h+\delta+\gamma_h)I_h - \rho_h E_h \\ (\mu_v+L_v)E_v \\ \mu_v I_v - L_v E_v \end{pmatrix} \tag{9}$$

The corresponding Jacobian matrices F and V of f and v are the linearisation of the system around E_0

$$F = \begin{pmatrix} 0 & 0 & 0 & \beta_1 a \\ 0 & 0 & 0 & 0 \\ 0 & \beta_2 ak\dfrac{\alpha_v\mu_h}{\alpha_h\theta_v} & 0 & 0 \\ 0 & 0 & 0 & 0 \end{pmatrix}, V = \begin{pmatrix} \rho_h+\mu_h & 0 & 0 & 0 \\ -\rho_h & \mu_h+\delta+\gamma_h & 0 & 0 \\ 0 & 0 & \mu_v+L_v & 0 \\ 0 & 0 & -L_v & \mu_v \end{pmatrix}. \tag{10}$$

This implies,

$$V^{-1} = \begin{pmatrix} \dfrac{1}{\rho_h+\mu_h} & 0 & 0 & 0 \\ \dfrac{\rho_h}{(\rho_h+\mu_h)(\mu_h+\delta+\gamma_h)} & \dfrac{1}{\mu_h+\delta+\gamma_h} & 0 & 0 \\ 0 & 0 & \dfrac{1}{\mu_v+L_v} & 0 \\ 0 & 0 & \dfrac{L_v}{\mu_v(\mu_v+L_v)} & \dfrac{1}{\mu_v} \end{pmatrix} \tag{11}$$

Then,

$$FV^{-1} = \begin{pmatrix} 0 & 0 & \dfrac{\beta_1 a L_v}{\mu_v(\mu_v+L_v)} & \dfrac{\beta_1 a}{\mu_v} \\ 0 & 0 & 0 & 0 \\ \dfrac{\beta_2 aK\alpha_v\mu_h\rho_h}{\theta_v\alpha_h(\rho_h+\mu_h)(\mu_h+\delta+\gamma_h)} & \dfrac{\beta_2 aK\alpha_v\mu_h}{\theta_v\alpha_h(\mu_h+\delta+\gamma_h)} & 0 & 0 \\ 0 & 0 & 0 & 0 \end{pmatrix} \tag{12}$$

And, the dominant eigenvalue of FV^{-1} defined as the reproduction number, is given by

$$R_0 = \sqrt{\frac{\beta_1\beta_2 a^2 K\alpha_v\rho_h\mu_h L_v}{\theta_v\alpha_h\mu_v(\rho_h+\mu_h)(\mu_h+\delta+\gamma_h)(\mu_v+L_v)}}. \tag{13}$$

□

Lemma 2.4. *The DFE* E_0 *is locally asymptotically stable if* $R_0 < 1$ *and unstable if* $R_0 > 1$.

Proof. The proof of this lemma is provided in [33]. □

2.2.3. Existence of Endemic Equilibrium Point

In order to find the model's endemic equilibrium point $\left(S_h^*, E_h^*, I_h^*, R_h^*, S_v^*, E_v^*, I_v^*\right)$, that is equilibrium points when at least one of the infected components is non-zero, we set the right-hand sides of system (1) equal to zero. Once we've set the derivatives to zero, we solve the resulting equations to determine the values of the compartments at the endemic equilibrium. At this equilibrium, the force of infection for humans, denoted as λ_h^*, and the force of infection for vectors, denoted as λ_v^*, will play a critical role. These forces of infection represent the rate at which susceptible individuals become infected by the disease in the endemic state.

The terms of force infections and the total human population in the endemic states are given by

$$\lambda_h^* = \frac{\beta_1 a I_v^*}{N_h^*}, \tag{14}$$

$$\lambda_v^* = \frac{\beta_1 a I_h^*}{N_h^*}, \tag{15}$$

$$N_h^* = S_h^* + E_h^* + I_h^* + R_h^*. \tag{16}$$

Solving the equations, we get

$$S_h^* = \frac{a_1 b_1 c_1 \alpha_h}{a_1 b_1 c_1\left(\lambda_h^* + \mu_h\right) - q\gamma_h\lambda_h^*\rho_h},$$

$$E_h^* = \frac{b_1 c_1 \alpha_h \lambda_h^*}{a_1 b_1 c_1\left(\lambda_h^* + \mu_h\right) - q\gamma_h\lambda_h^*\rho_h},$$

$$I_h^* = \frac{c_1 \alpha_h \lambda_h^* \rho_h}{a_1 b_1 c_1\left(\lambda_h^* + \mu_h\right) - q\gamma_h\lambda_h^*\rho_h},$$

$$R_h^* = \frac{\alpha_h\gamma_h\lambda_h^*\rho_h}{a_1 b_1 c_1\left(\lambda_h^* + \mu_h\right) - q\gamma_h\lambda_h^*\rho_h}, \tag{17}$$

$$S_v^* = \frac{d_1 K\mu_v\left(\mu_v\left(d_1\left(\theta_v - \lambda_v^* - \mu_v\right) + \theta_v\lambda_v^*\right) + L_v\theta_v\lambda_v^*\right)}{\theta_v\left(\mu_v\left(d_1 + \lambda_v^*\right) + L_v\lambda_v^*\right)^2},$$

$$E_v^* = \frac{K\lambda_v^*\mu_v\left(\mu_v\left(d_1\left(\theta_v - \lambda_v^* - \mu_v\right) + \theta_v\lambda_v^*\right) + L_v\theta_v\lambda_v^*\right)}{\theta_v\left(\mu_v\left(d_1 + \lambda_v^*\right) + L_v\lambda_v^*\right)^2},$$

$$I_v^* = \frac{KL_v\lambda_v^*\left(\mu_v\left(d_1\left(\theta_v - \lambda_v^* - \mu_v\right) + \theta_v\lambda_v^*\right) + L_v\theta_v\lambda_v^*\right)}{\theta_v\left(\mu_v\left(d_1 + \lambda_v^*\right) + L_v\lambda_v^*\right)^2},$$

where $a_1 = \rho_h + \mu_h, b_1 = \mu_h + \gamma_h + \delta, c_1 = \mu_h + q, d_1 = \mu_v + L_v$.

We got the following polynomial function in terms of λ_h^* by substituting Equations (17), (15) and (16) into Equation (14),

$$f\left(\lambda_h^*\right) = \left(A_3\lambda_h^{*3} + A_2\lambda_h^{*2} + A_1\lambda_h^* + A_0\right) \tag{18}$$

where A_i are given in the section of **Appendix D**. We show that there is possible existence of positive roots to Equation (18) by applying the concept of Descarte's rule of signs [34]. A_3 is always positive, while A_2 and A_1 can be either positive or negative, according to **Appendix D**. If $R_0 < 1$ then A_0 is positive and if $R_0 > 1$ then A_0 is negative. Table 3 provides an overview of Descartes's rule of signs [34].

Table 3. Possible number of positive roots of equation of (18).

A_3	A_2	A_1	A_0	Number of positive roots	R_0
+	+	+	+	0	$R_0 < 1$
+	+	-	+	2 or 0	$R_0 < 1$
+	-	+	+	2 or 0	$R_0 < 1$
+	-	-	+	2 or 0	$R_0 < 1$
+	+	+	-	1	$R_0 > 1$
+	+	-	-	1	$R_0 > 1$
+	-	+	-	3 or 1	$R_0 > 1$
+	-	-	-	1	$R_0 > 1$

Lemma 2.5 *If* $R_0 > 1$, *the model has at least one endemic point.*

3. Numerical Simulation

3.1. Parameter Estimation

In order to conduct numerical analysis, it is necessary to estimate and contextualize the model parameter values. The *Python* program was used for the numerical simulation process [35]. The specified temperature range of ([15˚C - 35˚C]) was used in the numerical simulation, it reflects the typical climate of Burundi. For rainfall, a range of ([0 - 50 mm]) was used, the 50 mm limit for rainfall serves as the threshold for flushing out mosquitoes when rainfall exceeds this value.

The total population in Burundi was 10,933,352 people in 2015. We consider a scenario in which the human population in this region has reached a steady state, which means that $\alpha_h/\mu_h = 10933352$, where α_h and μ_h represent respectively the birth rate and mortality rate of the humans population. To determine the mortality rate, we used the life expectancy of the population in 2015, which

was 60.22 years. Therefore, the mortality rate is given by $\mu_h = 1/60.22 \times 12$ per month. Consequently, the birth rate can be calculated as $\alpha_h = \mu_h \times 10933352 = 15129$.

Functions related to the climate, such as mosquito birth rate $\theta_v(T,R)$, biting rate $a(T)$, mortality rate $\mu_v(T)$ for mosquito and progression rate of mosquito population from E_v to I_v, $L_v(T)$ are detailed in **Appendix E**. These parameters have an impact on the activities that take place during both the aquatic and adult phases. For example, a sufficient amount of rainfall is necessary for the eggs, larvae, and pupae to survive, whereas temperature plays a significant role in the gonotrophic cycle, which is the period between a blood meal and the laying of eggs [23]. The values for the climate-related parameters are given in **Table 4**. We also show their references in the same table.

Table 4. Climate-related parameters.

Parameter	Value	Reference	Parameter	Value	Reference
A_1	0.000203	[36]	N_E	200	[23]
A_2	11.7	[36]	DD	111	[37]
A_3	42.3	[36]	K	100,000	[38]
A	−0.03	[23]	B	1.31	[23]
C	−4.4	[23]	χ_E	1	[23]
χ_p	1	[23]	$T_{\min}$	16	[37]

Model Fitting

We used cumulative monthly data of confirmed malaria cases from the year 2015 to the year 2022 to adjust the model. The parameter fitting was performed using the least square method. We defined the cumulative number of infected cases predicted by the model by

$$\frac{\mathrm{d}C_h(t)}{\mathrm{d}t} = \rho_h E_h(t), \tag{19}$$

where ρ_h is a parameter related to the rate at which exposed individuals become infectious, $C_h(t)$ is the cumulative number of infected cases at time t and $E_h(t)$ is the number of exposed individuals at time t. This equation indicates that the rate of change of the cumulative number of infected cases $C_h(t)$ depends on the number of exposed individuals and the rate at which they become infectious. The least square method was used to fit the model with the real infected data by minimizing the sum of the squares difference between the real data and the model (1) together with (19) [39]. It is calculated as follows:

$$\min_{\theta} \sum_{i=1}^{n} \left(y_i - F(x_i, \theta) \right)^2, \tag{20}$$

where n represents the total number of available data, y_i represents the cumulative number of the real reported data for the i^{th} observation and the function $F(x,\theta)$ is a function in the form of vectors with the same dimension as y. It

represents the model's predictions for the cumulative number of malaria cases at each observation point, given the parameters θ. The step for minimization can be found in [40].

The data used were given by the national malaria control program in Burundi. Parameter values calculated in Section 3.1 and Table 4 were used to generate Figure 2 and Table 5

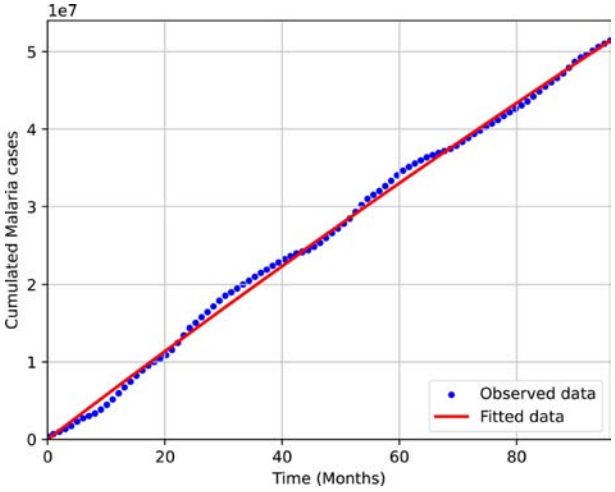

Figure 2. Model fit to data for malaria in Burundi.

Table 5 contains the fitted parameters.

Table 5. Outcomes of the data fitting on malaria in Burundi to the parameters.

Parameter	Value	Parameter	Value
q	0.98765	β_2	0.9917
δ	0.015941	γ_h	0.120342
β_1	0.9969	ρ_h	0.001995

3.2. Forward Sensitivity Analysis of the Reproduction Number

In this section, the forward normalized sensitivity index of the basic reproduction number R_0 is conducted to assess the sensitivity of the basic reproduction number with respect to various parameters of the model. The objective is to identify and understand the key factors that have a substantial impact on the basic reproduction number. For effective strategies in controlling and eradicating malaria, it is crucial to prioritize interventions targeting these influential factors. Sensitivity analysis involves examining how changes in specific parameters affect the overall value of R_0. If certain parameters have a pronounced effect on R_0, addressing or modifying those parameters can significantly impact the transmission dynamics of malaria.

Definition 3.1. *The sensitivity index* [41] *of a variable* x *with respect to a parameter* p *in the context of continuous dependence is expressed as*:

$$\Gamma_p^x = \frac{\partial x}{\partial p}\frac{p}{x}. \tag{21}$$

If we consider the sensitivity index of the basic reproduction number R_0 concerning the parameter β_1. It quantifies the degree to which variations in β_1 affect the potential for disease transmission, providing valuable insights into the significance of this specific parameter in influencing R_0. It is calculated as

$$\Gamma_{\beta_1}^{R_0} = \frac{\partial R_0}{\partial \beta_1}\frac{\beta_1}{R_0}, \tag{22}$$

whith

$$R_0 = \sqrt{\frac{\beta_1\beta_2 a^2(T)K\alpha_v\rho_h\mu_h KL_v(T)}{\theta_v(T,R)\alpha_h\mu_v(T)(\rho_h+\mu_h)(\mu_h+\delta+\gamma_h)(\mu_v(T)+L_v(T))}},$$

written in terms of climate-dependent parameters with $a(T), L_v(T), \mu_v(T), \theta_v(T,R)$ detailed in **Appendix E**. In sensitivity, Table 6 presents the sensitivity indices for R_0 concerning parameters in the model (1). Parameters from Table 4, Table 5 are used, and the sensitivity of temperature and rainfall are also shown in Figure 3. The results indicate that the parameters β_1, β_2, and K are strongly positively correlated with R_0. An increase in these parameters leads to a rise in R_0, highlighting the critical role of human-to-vector transmission in increasing R_0. This underscores the importance of controlling vector-to-human transmission to manage R_0. On the other hand, the rate of transition from infectious to recovered in the human population (γ_h) negatively impacts R_0. Increasing γ_h will decrease R_0. Thus, measures such as using bed nets and applying indoor and outdoor sprays can be effective in reducing malaria transmission. Finally, in Figure 3, we observed that the sensitivity indices of R_0 is increasing when temperatures are between 17˚C and 32˚C. This corresponds to the temperature ranges for disease transmission defined by [42]. Furthermore, as the amount of rainfall increases, the sensitivity to rainfall decreases. The mean monthly rainfall below 30 mm is associated with positive indices, whereas the mean monthly rainfall above is associated with negative indices.

Table 6. Sensitivity indices of R_0.

Parameter symbol	Sensitivity indices of R_0
β_1	0.6346
μ_h	0.1296
ρ_h	0.4779
γ_h	−0.5364
δ	−0.0710
K	0.6360
β_2	0.6346

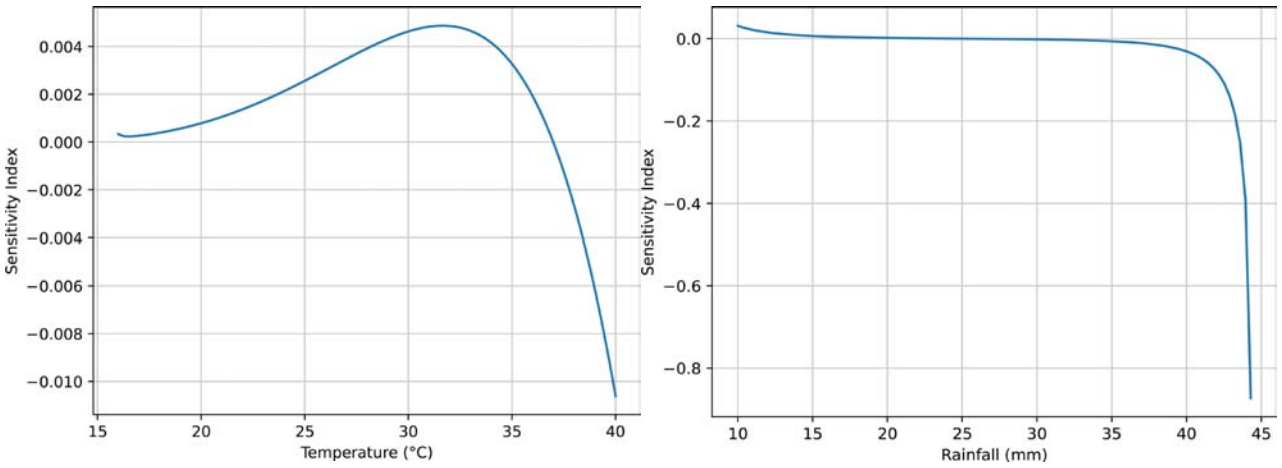

(a) (b)

Figure 3. Sensitivity indices of the reproduction number with respect to temperature and rainfall.

3.3. Vector Population Dynamics and Climate-Related Parameters

In this section, we show how temperature and rainfall affect the transmission dynamics of malaria.

Figure 4 and Figure 5 provide insights into various aspects of mosquito behavior. In Figure 4, the mosquito biting rate, mosquito parasite development, and mosquito mortality rate are presented against mean monthly temperatures from 10˚C to 40˚C.

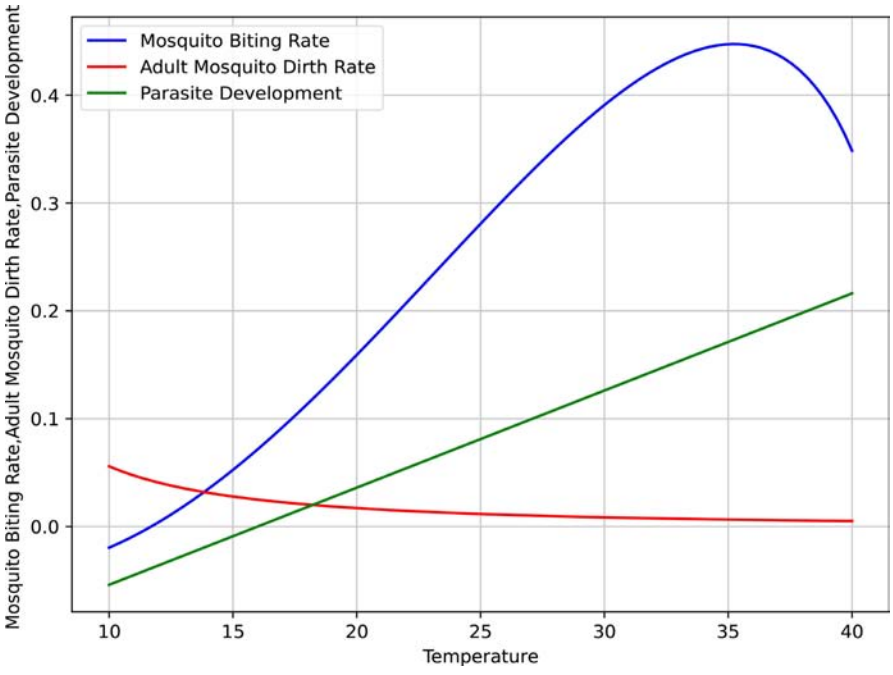

Figure 4. Temperature-dependent functions in mosquito modelling.

Figure 5 illustrates the birth rate of mosquitoes, a parameter influenced by temperature and rainfall, in relation to mean monthly temperatures (10˚C - 40˚C)

and mean monthly rainfall values (0 - 50 mm). We also plot the reproduction number as a function of temperature and rainfall Figure 6. These findings suggest that the optimal conditions for the mosquito population fall within the temperature range of 20 ˚C - 32˚C and a rainfall range of 10 - 30 mm, with the same results for reproduction number.

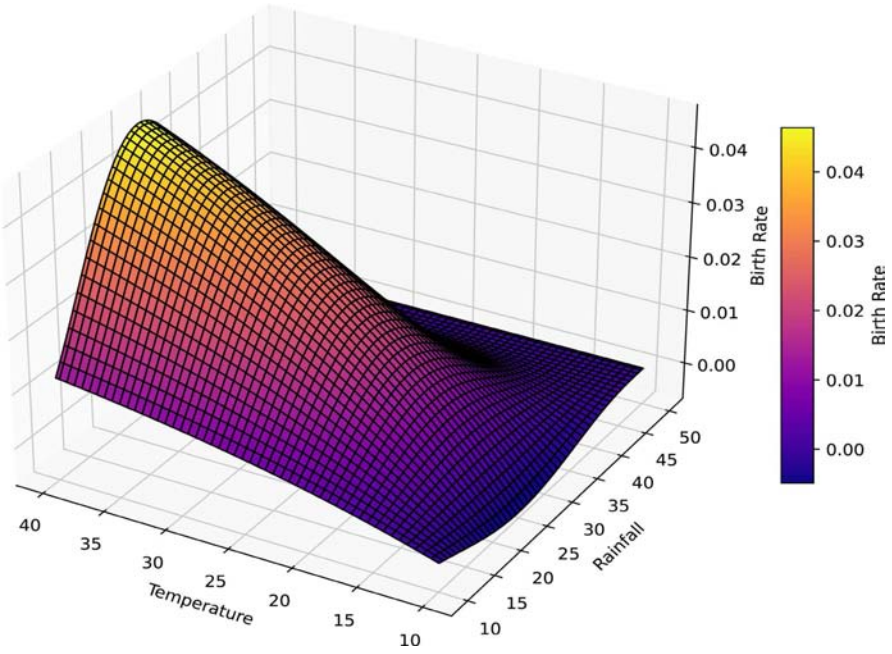

Figure 5. Mosquito birth rate plotted against temperature and rainfall.

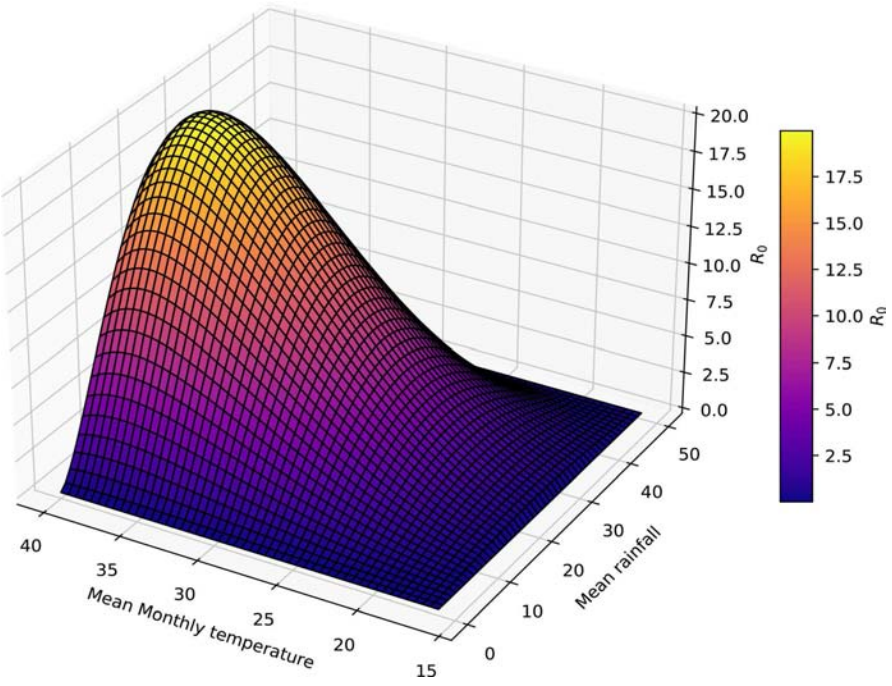

Figure 6. Reproduction numbers are plotted against mean monthly temperature and mean monthly rainfall.

To show the influence of temperature, we conducted simulations on the mosquito model under varying temperatures while keeping rainfall constant at 25 mm (See Figure 7). Temperature values of $T = 20^{\circ}C$, $25^{\circ}C$, $30^{\circ}C$, and $35^{\circ}C$ were used in the analysis. The results indicate a consistent decrease in the simulation of susceptible mosquitoes across all temperature values (Figure 7(a)). Notably, Figure 7(b) and Figure 7(c) illustrate the dynamics of exposed and infected mosquito classes exhibit the highest rate of increase at a temperature of $20^{\circ}C$, while the lowest rate is observed at $35^{\circ}C$. This aligns with the findings obtained from the sensitivity analysis of temperature and rainfall, suggesting a correlation between temperature levels and the transmission dynamics of malaria.

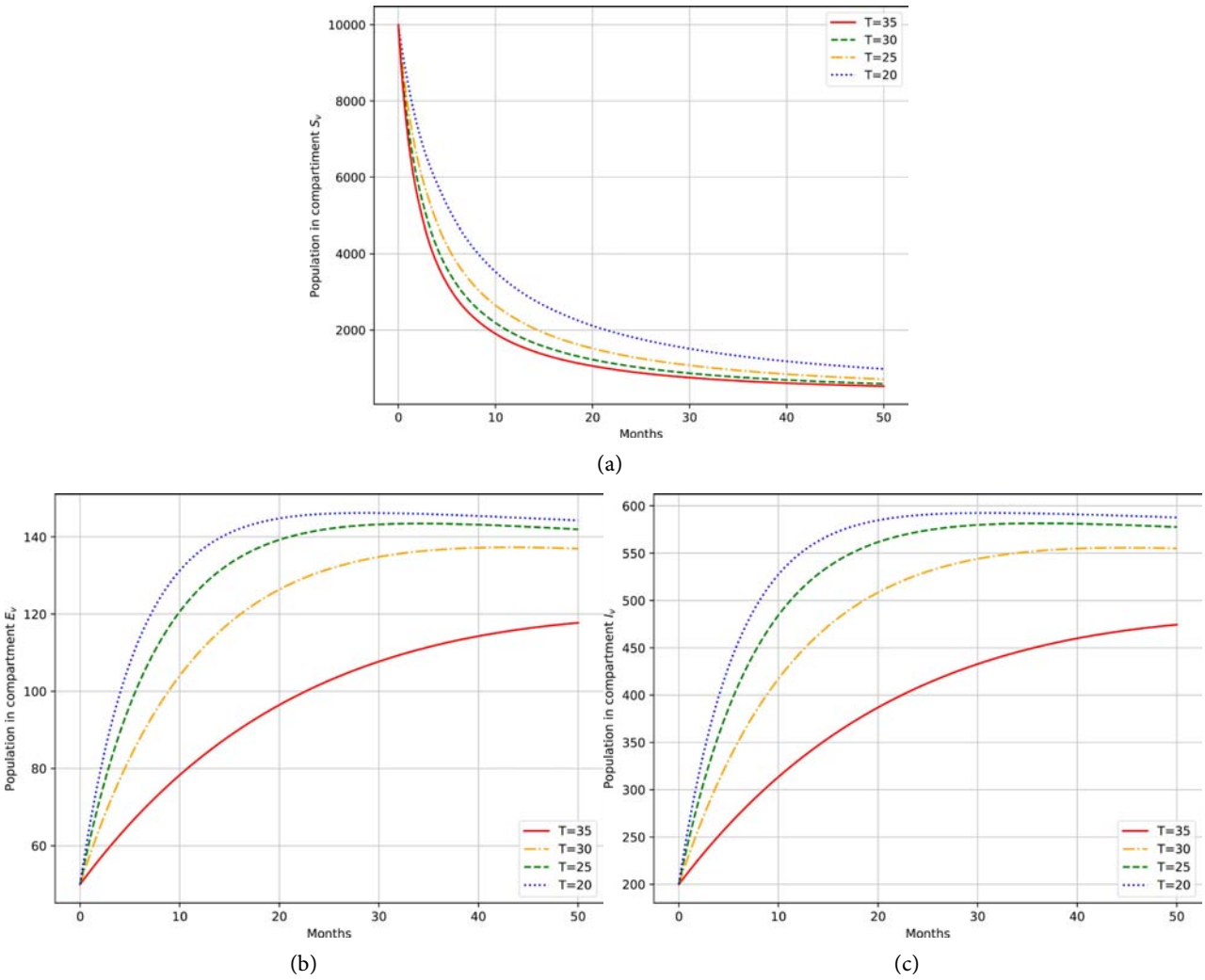

Figure 7. Variations in mosquito population across time at different temperature levels, with (a) susceptible, (b) exposed, and (c) infected mosquitoes.

We also explored the influence of rainfall while keeping the temperature constant at $T = 20^{\circ}C$ (see Figure 8). We observe that the susceptible class consistently decreased as rainfall increased from 10 to 45 mm, indicating a negative effect on

susceptible mosquito population Figure 8(a). In contrast, both the exposed and infected classes exhibited an upward trend with time and a decrease after a certain time (Figure 8(b), Figure 8(c)). The lowest graph was associated with a rainfall of 45 mm, while the highest was observed at 20 mm, coinciding with the results at 30 mm. Consequently, it can be inferred that the optimal range for mosquito proliferation lies within the rainfall range of 10 to 30 mm. Excessive rainfall may disrupt breeding sites and reduce the susceptible mosquito population, while moderate rainfall supports mosquito reproduction. The infection rate of malaria varies depending on the amount of rainfall, indicating that rainfall has an impact on the transmission of the disease. Different levels of rainfall can influence the breeding and survival of mosquitoes, which are the primary vectors for transmitting malaria.

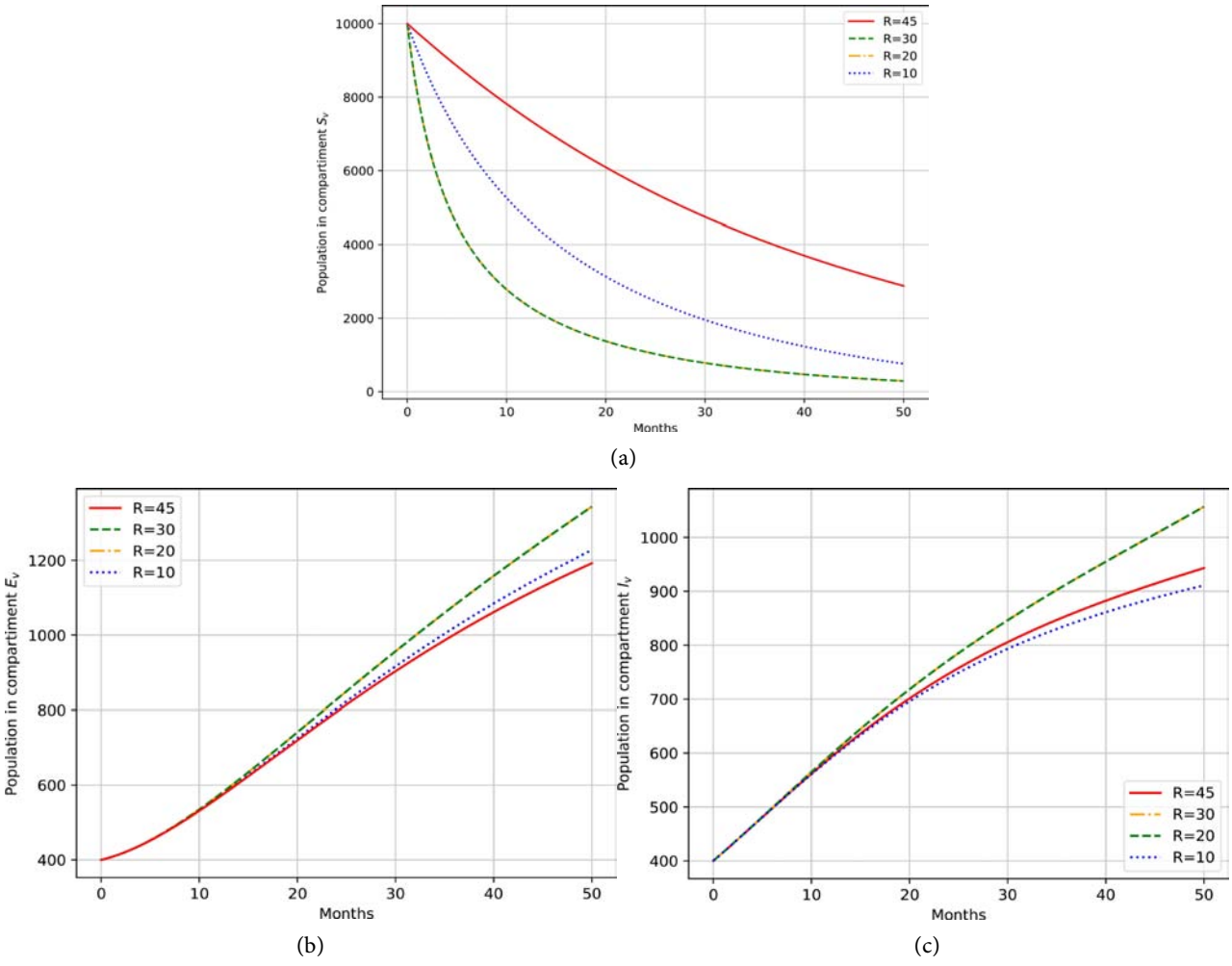

Figure 8. Variations in mosquito population across time at different rainfall levels, with (a) susceptible, (b) exposed, and (c) infected mosquitoes.

3.4. Monthly Trends in Temperature, Rainfall, and Confirmed Malaria

For a better understanding, temperature and rainfall data were analyzed alongside

percentage of confirmed malaria cases using the data between the year 2015-2022. Graphical representations were used to visualize the relationship between temperature, rainfall, and malaria cases. Additionally, the variation of the reproduction number (R_0) was calculated, and we plotted this on a monthly basis to include the percentage of confirmed malaria cases.

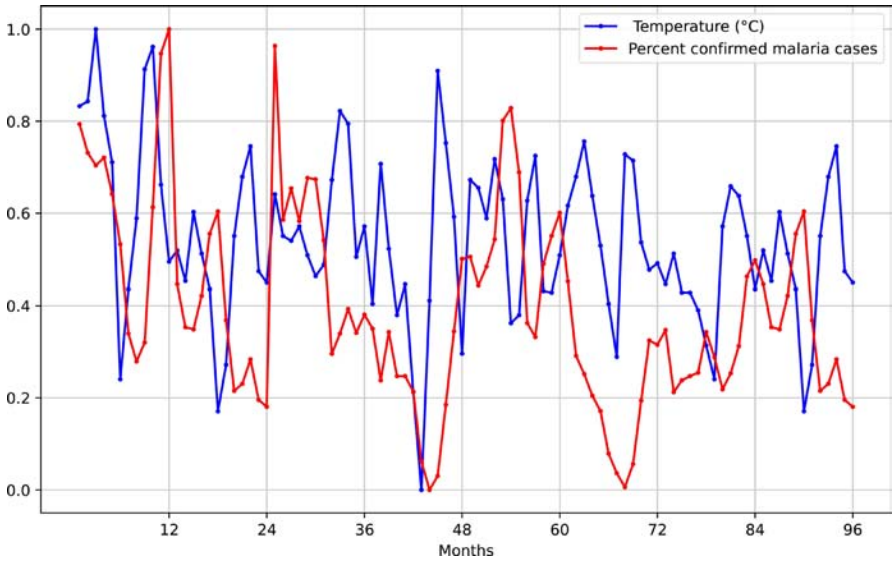

Figure 9. Monthly temperature and confirmed malaria percent.

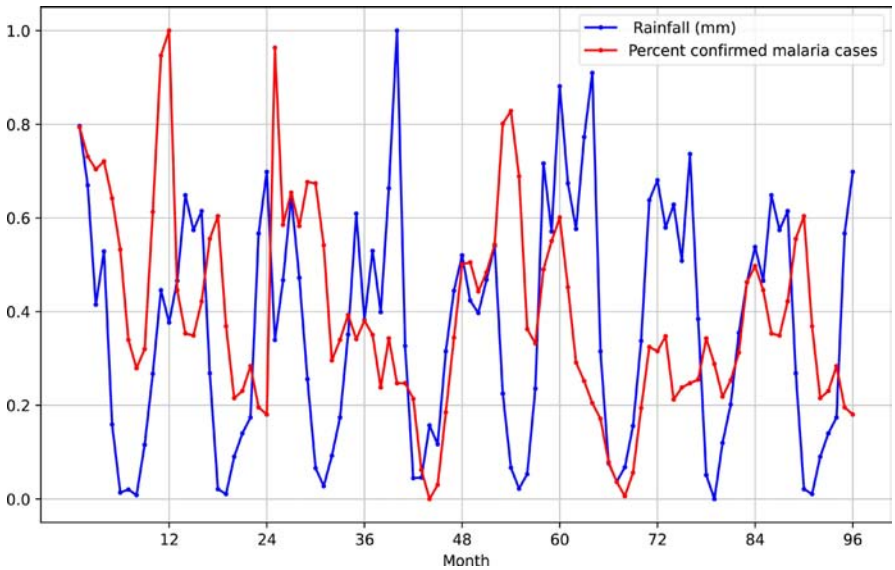

Figure 10. Monthly rainfall and confirmed malaria percent.

We notice that when rainfall reaches its highest point in a given month, malaria does not immediately peak during that same month (See Figure 10). Similarly, when rainfall decreases in a month, malaria rates drop after a period of time. This indicates that alterations in rainfall patterns eventually lead to corresponding changes in malaria occurrence, with the impact becoming evident after some time.

We observed same behaviour when we plot mean monthly temperature against the monthly confirmed malaria percent (see Figure 9). We observed a similar analysis when we computed the reproduction number and plotted it against confirmed malaria percent, as shown in Figure 11. This is because the reproduction number is influenced by temperature and rainfall.

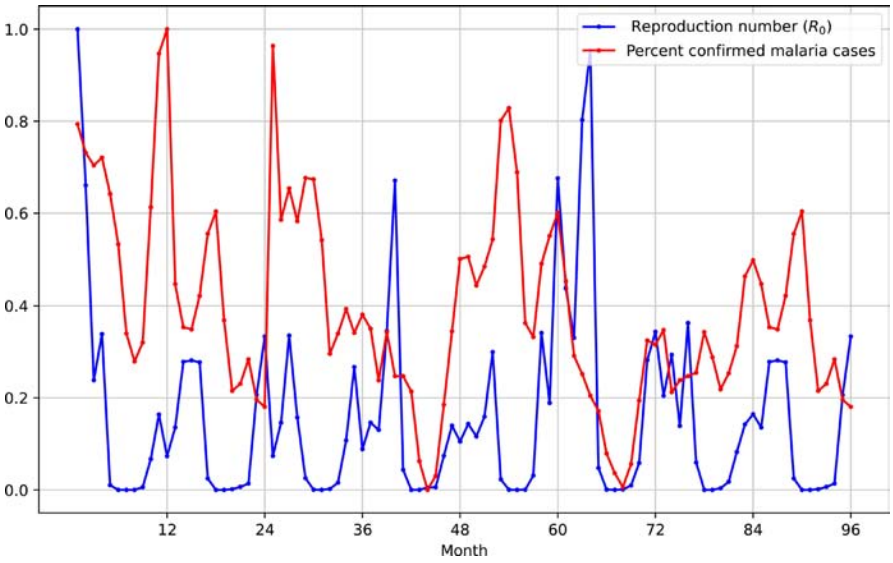

Figure 11. Reproduction number and monthly confirmed malaria percent.

4. Discussion

In this research, we presented a mathematical model that captures the dynamics of malaria transmission, incorporating temperature and rainfall as climate-dependent parameters. Our analysis indicated that the model is well-defined both mathematically and epidemiologically. Upon further investigation, we observed that the model possesses a disease-free equilibrium point and exhibits local stability when the basic reproduction number $R_0 < 1$. Additionally, the basic reproduction number is computed using the next-generation matrix. We conducted computations to establish the existence of an endemic equilibrium point and found that the model will have at least one endemic equilibrium point when $R_0 > 1$, this implies that malaria persists within the community as long as R_0 remains greater than 1.

We used the least square method to verify the accuracy of the model by fitting the cumulative incidence of (19) with cumulative observed malaria cases data for Burundi. Through curve fitting, we derived specific parameters, which were subsequently employed in our simulations Table 5. A sensitivity analysis was conducted to elucidate the significance of various parameters in influencing the reproduction number. The outcomes of this analysis have been systematically presented in sensitivity Table 6. We observe that human-mosquito contact is among the primary parameters exhibiting a significant positive influence on the reproduction number (R_0). Consequently, implementing strategies like distributing

bed nets for sleeping and conducting indoor and outdoor mosquito spraying can effectively reduce the contact between humans and mosquitoes and subsequently reducing the transmission of malaria.

Additionally, sensitivity analysis were extended to assess the impact of temperature and rainfall (See **Figure 3**), aiming to identify optimal values conducive to the proliferation of mosquitoes and, subsequently, the transmission of malaria. The range of temperature from 20˚C to 32 ˚C and rainfall ranging from 10 to 30 mm through the month proves to be particularly favorable for the development of mosquitoes, as illustrated in **Figure 7** and **Figure 8**. This observation emphasizes the considerable impact of warm weather ecology on the dynamics of mosquitoes and identifies a specific range of temperature and rainfall that can create favorable conditions for mosquitoes in Burundi and potentially in other regions with similar epidemiological and climatic characteristics. These results align consistently with findings from multiple studies [38] [42]. Consequently, it becomes imperative to understand the repercussions of climate factors on the transmission dynamics of malaria, as such insights are essential for formulating effective strategies to combat the spread of malaria.

The model underwent numerical simulations to examine the impact of temperature and rainfall on malaria transmission. Temperature values ranging from 20˚C to 35˚C were explored, revealing that malaria transmission is most effective in the range of [20˚C - 32˚C] and a rainfall range of [10 mm - 30 mm]. It was observed that rainfall of 20 mm to 30 mm is conducive to optimal malaria transmission in accordance with [24].

In areas with low rainfall, the breeding sites for mosquitoes may dry up, reducing their population and consequently lowering the transmission of malaria. On the other hand, excessive rainfall can create stagnant water bodies, providing abundant breeding grounds for mosquitoes and increasing the transmission of the disease. Additionally, excessive rainfall exceeding 50 mm can contribute to a decline in the mosquito population by flushing them out of their habitats. Comparing monthly confirmed malaria percentages to the average monthly rainfall and temperature revealed that the effects on malaria occurrence were observed in subsequent months rather than immediately in the same month. Changes in these climatic factors led to delayed impacts on malaria transmission. This finding aligns with similar conclusions reported by [43] [44], both of which highlight the seasonality of malaria transmission and the delayed response to climate variables. In a related study conducted in North Kordofan State, Sudan, a regression model found that 72% of the variance in monthly malaria incidence could be explained by climate factors, with lagged malaria cases and temperature (particularly minimum temperature) serving as key predictors. The study emphasized a peak in malaria cases during the rainy season (June to September) but noted a lagged effect similar to our findings, where changes in rainfall and temperature influenced malaria transmission after a certain delay [45].

The implication for future research is that it would be beneficial to delve deeper

into the seasonal patterns of malaria transmission. Seasonal analysis allows for a more comprehensive understanding of how changes in climatic variables, such as temperature and rainfall, as well as other factors, such as relative humidity, wind speed, and vegetation indices, influence malaria incidence over time. Including a broader range of variables can provide a more detailed picture of the environmental drivers of malaria, ultimately aiding in the development of more effective intervention strategies.

Acknowledgements

The authors thank the interdisciplinary research program of the Doctoral School of the University of Burundi (Burundi) for its kind collaboration. KJGS appreciates the generous funding from the Organization for Women in Science for the Developing World (OWSD). This work was carried out with the support of OWSD and the Swedish International Development Cooperation Agency (SIDA).

Conflicts of Interest

The authors declare no conflicts of interest regarding the publication of this paper.

References

[1] Encyclopaedia Britannica Inc, *et al.* (1993) Encyclopædia britannica.

[2] Concern Worldwide (2024) Where We Work: Burundi.

[3] World Health Organization (2020) World Malaria Report 2020: 20 Years of Global Progress and Challenges.

[4] Djihinto, O.Y., Medjigbodo, A.A., Gangbadja, A.R.A., Saizonou, H.M., Lagnika, H.O., Nanmede, D., *et al.* (2022) Malaria-Transmitting Vectors Microbiota: Overview and Interactions with Anopheles Mosquito Biology. *Frontiers in Microbiology*, **13**, Article 891573. https://doi.org/10.3389/fmicb.2022.891573

[5] Moravec, F. (2010) Gibbons LM: Keys to the Nematode Parasites of Vertebrates. Supplementary Volume. *Parasites & Vectors*, **3**, Article No. 9. https://doi.org/10.1186/1756-3305-3-9

[6] Martens, W., Jetten, T., Rotmans, J. and Niessen, L. (1995) Climate Change and Vector-Borne Diseases. *Global Environmental Change*, **5**, 195-209. https://doi.org/10.1016/0959-3780(95)00051-o

[7] Alemu, A., Abebe, G., Tsegaye, W. and Golassa, L. (2011) Climatic Variables and Malaria Transmission Dynamics in Jimma Town, South West Ethiopia. *Parasites & Vectors*, **4**, Article No. 30. https://doi.org/10.1186/1756-3305-4-30

[8] IHME (2020) Health Metrics for Burundi. https://www.healthdata.org/burundi

[9] Lok, P. and Dijk, S. (2019) Malaria Outbreak in Burundi Reaches Epidemic Levels with 5.7 Million Infected This Year. *British Medical Journal*, **366**, Article 15104. https://doi.org/10.1136/bmj.l5104

[10] World Vision Burundi (2017) Eight Facts about Burundi's Malaria Epidemic. https://www.wvi.org/article/8-facts-about-burundis-malaria-epidemic

[11] Ngarakana-Gwasira, E.T., Bhunu, C.P., Masocha, M. and Mashonjowa, E. (2016) Assessing the Role of Climate Change in Malaria Transmission in Africa. *Malaria Research and Treatment*, **2016**, 1-7. https://doi.org/10.1155/2016/7104291

[12] Lahondère, C., Vinauger, C., Liaw, J.E., Tobin, K.K.S., Joiner, J.M. and Riffell, J.A. (2023) Effect of Temperature on Mosquito Olfaction. *Integrative and Comparative Biology*, **63**, 356-367. https://doi.org/10.1093/icb/icad066

[13] Tolle, M.A. (2009) Mosquito-Borne Diseases. *Current Problems in Pediatric and Adolescent Health Care*, **39**, 97-140. https://doi.org/10.1016/j.cppeds.2009.01.001

[14] Gubler, D.J., Reiter, P., Ebi, K.L., Yap, W., Nasci, R. and Patz, J.A. (2001) Climate Variability and Change in the United States: Potential Impacts on Vector and Rodent-Borne Diseases. *Environmental Health Perspectives*, **109**, 223-233. https://doi.org/10.1289/ehp.109-1240669

[15] Mabaso, M.L.H., Craig, M., Ross, A. and Smith, T. (2007) Environmental Predictors of the Seasonality of Malaria Transmission in Africa: The Challenge. *The American Journal of Tropical Medicine and Hygiene*, **76**, 33-38. https://doi.org/10.4269/ajtmh.2007.76.33

[16] Githeko, A.K., Lindsay, S.W., Confalonieri, U.E. and Patz, J.A. (2000) Climate Change and Vector-Borne Diseases: A Regional Analysis. *Bulletin of the World Health Organization*, **78**, 1136-1147.

[17] McKenzie, F.E. (2000) Why Model Malaria? *Parasitology Today*, **16**, 511-516. https://doi.org/10.1016/s0169-4758(00)01789-0

[18] Ronald, R. (1911) The Prevention of Malaria. John Murray.

[19] Anderson, R.M. and May, R.M. (1992) Infectious Diseases of Humans: Dynamics and Control. Oxford University Press.

[20] Koella, J.C. and Boëte, C. (2003) A Model for the Coevolution of Immunity and Immune Evasion in Vector-Borne Diseases with Implications for the Epidemiology of Malaria. *The American Naturalist*, **161**, 698-707. https://doi.org/10.1086/374202

[21] Kribs-Zaleta, C.M. and Martcheva, M. (2002) Vaccination Strategies and Backward Bifurcation in an Age-Since-Infection Structured Model. *Mathematical Biosciences*, **177**, 317-332. https://doi.org/10.1016/s0025-5564(01)00099-2

[22] Macdonald, G., *et al.* (1957) The Epidemiology and Control of Malaria.

[23] Parham, P.E. and Michael, E. (2010) Modeling the Effects of Weather and Climate Change on Malaria Transmission. *Environmental Health Perspectives*, **118**, 620-626. https://doi.org/10.1289/ehp.0901256

[24] Yiga, V., Nampala, H. and Tumwiine, J. (2020) Analysis of the Model on the Effect of Seasonal Factors on Malaria Transmission Dynamics. *Journal of Applied Mathematics*, **2020**, 1-19. https://doi.org/10.1155/2020/8885558

[25] Mafwele, B.J. and Lee, J.W. (2022) Relationships between Transmission of Malaria in Africa and Climate Factors. *Scientific Reports*, **12**, Article No. 14392. https://doi.org/10.1038/s41598-022-18782-9

[26] Hay, S.I., Cox, J., Rogers, D.J., Randolph, S.E., Stern, D.I., Shanks, G.D., *et al.* (2002) Climate Change and the Resurgence of Malaria in the East African Highlands. *Nature*, **415**, 905-909. https://doi.org/10.1038/415905a

[27] Sakubu, D., Sinigirira, K.J.G. and Niyukuri, D. (2024) Predicting Malaria Dynamics in Burundi Using Deep Learning Models. *Journal of Applied Mathematics and Physics*, **12**, 2904-2917. https://doi.org/10.4236/jamp.2024.128173

[28] Ndamuzi, E. and Gahungu, P. (2021) Mathematical Modeling of Malaria Transmission Dynamics: Case of Burundi. *Journal of Applied Mathematics and Physics*, **9**, 2447-2460. https://doi.org/10.4236/jamp.2021.910156

[29] Lim, A., Cheong, H., Chung, Y., Sim, K. and Kim, J. (2021) Mosquito Abundance in

Relation to Extremely High Temperatures in Urban and Rural Areas of Incheon Metropolitan City, South Korea from 2015 to 2020: An Observational Study. *Parasites & Vectors*, **14**, Article No. 559. https://doi.org/10.1186/s13071-021-05071-z

[30] Berselli, L.C. (2021) Three-Dimensional Navier-Stokes Equations for Turbulence. Academic Press.

[31] Mandal, S., Sarkar, R.R. and Sinha, S. (2011) Mathematical Models of Malaria—A Review. *Malaria Journal*, **10**, Article No. 202. https://doi.org/10.1186/1475-2875-10-202

[32] van den Driessche, P. (2017) Reproduction Numbers of Infectious Disease Models. *Infectious Disease Modelling*, **2**, 288-303. https://doi.org/10.1016/j.idm.2017.06.002

[33] van den Driessche, P. and Watmough, J. (2002) Reproduction Numbers and Sub-Threshold Endemic Equilibria for Compartmental Models of Disease Transmission. *Mathematical Biosciences*, **180**, 29-48. https://doi.org/10.1016/s0025-5564(02)00108-6

[34] Anderson, B., Jackson, J. and Sitharam, M. (1998) Descartes' Rule of Signs Revisited. *The American Mathematical Monthly*, **105**, 447-451. https://doi.org/10.1080/00029890.1998.12004907

[35] Python Version 3.6.5.

[36] Paaijmans, K.P., Cator, L.J. and Thomas, M.B. (2013) Temperature-Dependent Pre-Bloodmeal Period and Temperature-Driven Asynchrony between Parasite Development and Mosquito Biting Rate Reduce Malaria Transmission Intensity. *PLOS ONE*, **8**, e55777. https://doi.org/10.1371/journal.pone.0055777

[37] Craig, M.H., Snow, R.W. and le Sueur, D. (1999) A Climate-Based Distribution Model of Malaria Transmission in Sub-Saharan Africa. *Parasitology Today*, **15**, 105-111. https://doi.org/10.1016/s0169-4758(99)01396-4

[38] Abiodun, G.J., Njabo, K.Y., Witbooi, P.J., Adeola, A.M., Fuller, T.L., Okosun, K.O., *et al.* (2018) Exploring the Influence of Daily Climate Variables on Malaria Transmission and Abundance of *Anopheles arabiensis* over Nkomazi Local Municipality, Mpumalanga Province, South Africa. *Journal of Environmental and Public Health*, **2018**, 1-10. https://doi.org/10.1155/2018/3143950

[39] Kamrujjaman, M., Saha, P., Islam, M.S. and Ghosh, U. (2022) Dynamics of SEIR Model: A Case Study of COVID-19 in Italy. *Results in Control and Optimization*, **7**, Article 100119. https://doi.org/10.1016/j.rico.2022.100119

[40] Martcheva, M. (2015) An Introduction to Mathematical Epidemiology. Springer.

[41] Rodrigues, H.S., Monteiro, M.T.T. and Torres, D.F.M. (2013) Sensitivity Analysis in a Dengue Epidemiological Model. *Conference Papers in Mathematics*, **2013**, 1-7. https://doi.org/10.1155/2013/721406

[42] Ngarakana-Gwasira, E.T., Bhunu, C.P. and Mashonjowa, E. (2013) Assessing the Impact of Temperature on Malaria Transmission Dynamics. *Afrika Matematika*, **25**, 1095-1112. https://doi.org/10.1007/s13370-013-0178-y

[43] Ikeda, T., Behera, S.K., Morioka, Y., Minakawa, N., Hashizume, M., Tsuzuki, A., *et al.* (2017) Seasonally Lagged Effects of Climatic Factors on Malaria Incidence in South Africa. *Scientific Reports*, **7**, Article No. 2458. https://doi.org/10.1038/s41598-017-02680-6

[44] Tigu, F., Gebremaryam, T. and Desalegn, A. (2021) Seasonal Profile and Five-Year Trend Analysis of Malaria Prevalence in Maygaba Health Center, Welkait District, Northwest Ethiopia. *Journal of Parasitology Research*, **2021**, 1-7. https://doi.org/10.1155/2021/6727843

[45] Hussien, H.H. (2020) Modeling the Influence of Climate Factors on Malaria Transmission Dynamics in North Kordofan State, Sudan. *Advances in Infectious Diseases*, **10**, 189-199. https://doi.org/10.4236/aid.2020.105017

[46] Jepson, W.F., Moutia, A. and Courtois, C. (1947) The Malaria Problem in Mauritius: The Bionomics of Mauritian Anophelines. *Bulletin of Entomological Research*, **38**, 177-208. https://doi.org/10.1017/s0007485300030273

[47] Shapiro, L.L.M., Whitehead, S.A. and Thomas, M.B. (2017) Quantifying the Effects of Temperature on Mosquito and Parasite Traits that Determine the Transmission Potential of Human Malaria. *PLOS Biology*, **15**, e2003489. https://doi.org/10.1371/journal.pbio.2003489

[48] Tesla, B., Demakovsky, L.R., Mordecai, E.A., Ryan, S.J., Bonds, M.H., Ngonghala, C.N., *et al.* (2018) Temperature Drives Zika Virus Transmission: Evidence from Empirical and Mathematical Models. *Proceedings of the Royal Society B: Biological Sciences*, **285**, Article 20180795. https://doi.org/10.1098/rspb.2018.0795

Appendices

A. Malaria Cases Data (Figure A1)

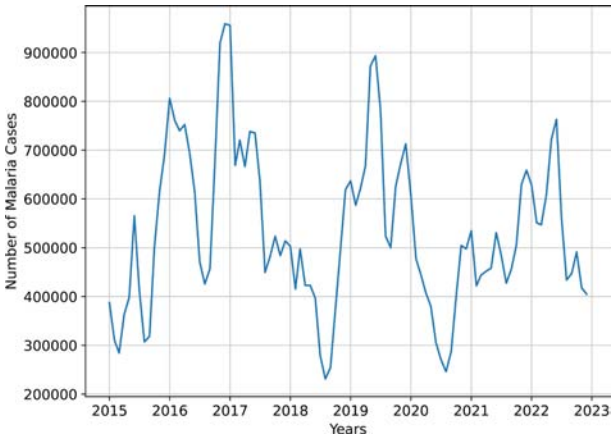

Figure A1. Monthly malaria cases from 2015 to 2022.

B. Temperature Data (Figure A2)

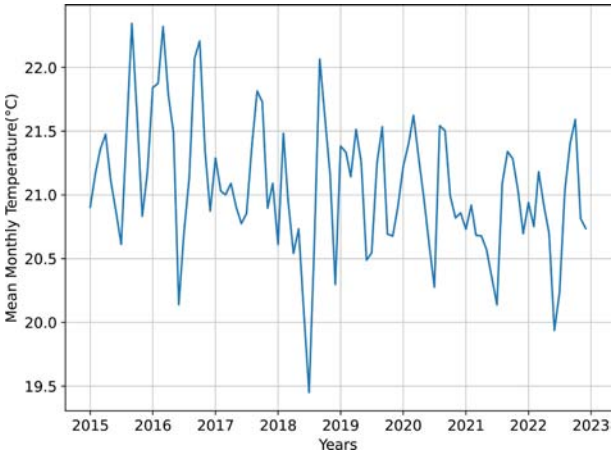

Figure A2. The average temperature per month from 2015 to 2022.

C. Rainfall Data Figure (Figure A3)

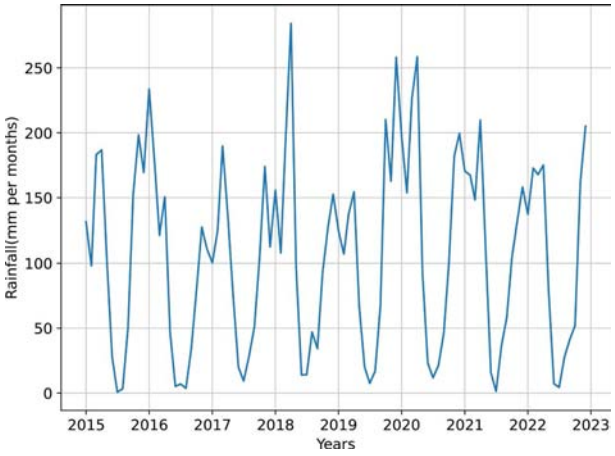

Figure A3. The total rainfall per month from 2015 to 2022.

D. Existence of EE

$$f\left(\lambda_h^*\right) = A_3\lambda_h^{*3} + A_2\lambda_h^{*2} + A_1\lambda_h^* + A_0 \tag{23}$$

where

$$\begin{aligned}
A_3 &= a^2\alpha_h\beta_1^2\theta_v\mu_v^2\rho_h^3c_1^3 + d_1^2\alpha_h\theta_v\mu_v^2\rho_h^3c_1^3 + 2ad_1\alpha_h\beta_1\theta_v\mu_v^2\rho_h^3c_1^3 + a^2L_v^2\alpha_h\beta_1^2\theta_v\rho_h^3c_1^3 \\
&+ 2ad_1L_v\alpha_h\beta_1\theta_v\mu_v\rho_h^3c_1^3 + b_1^3d_1^2\alpha_h\theta_v\mu_v^2c_1^3 + a^2b_1\alpha_h\beta_1^2\theta_v\mu_v^2\rho_h^2c_1^3 \\
&+ 3b_1d_1^2\alpha_h\theta_v\mu_v^2\rho_h^2c_1^3 + a^2b_1L_v^2\alpha_h\beta_1^2\theta_v\rho_h^2c_1^3 + 2a^2b_1L_v\alpha_h\beta_1^2\theta_v\mu_v\rho_h^2c_1^3 \\
&+ 4ab_1d_1L_v\alpha_h\beta_1\theta_v\mu_v\rho_h^2c_1^3 + 3b_1^2d_1^2\alpha_h\theta_v\mu_v^2\rho_hc_1^3 + 2ab_1^2d_1L_v\alpha_h\beta_1\theta_v\mu_v\rho_hc_1^3 \\
&+ a^2\alpha_h\beta_1^2\gamma_h\theta_v\mu_v^2\rho_h^3c_1^2 + 3d_1^2\alpha_h\gamma_h\theta_v\mu_v^2\rho_h^3c_1^2 + 4ad_1\alpha_h\beta_1\gamma_h\theta_v\mu_v^2\rho_h^3c_1^2 \\
&+ 2a^2L_v\alpha_h\beta_1^2\gamma_h\theta_v\mu_v\rho_h^3c_1^2 + 4ad_1L_v\alpha_h\beta_1\gamma_h\theta_v\mu_v\rho_h^3c_1^2 + 6b_1d_1^2\alpha_h\gamma_h\theta_v\mu_v^2\rho_h^2c_1^2 \\
&+ 4ab_1d_1L_v\alpha_h\beta_1\gamma_h\theta_v\mu_v\rho_h^2c_1^2 + 3b_1^2d_1^2\alpha_h\gamma_h\theta_v\mu_v^2\rho_hc_1^2 + 3d_1^2\alpha_h\gamma_h^2\theta_v\mu_v^2\rho_h^3c_1 \\
&+ 2ad_1\alpha_h\beta_1\gamma_h^2\theta_v\mu_v^2\rho_h^3c_1 + 2ad_1L_v\alpha_h\beta_1\gamma_h^2\theta_v\mu_v\rho_h^3c_1 + 3b_1d_1^2\alpha_h\gamma_h^2\theta_v\mu_v^2\rho_h^2c_1 \\
&+ d_1^2\alpha_h\gamma_h^3\theta_v\mu_v^2\rho_h^3 + 2a^2L_v\alpha_h\beta_1^2\theta_v\mu_v\rho_h^3c_1^3 + 4ab_1d_1\alpha_h\beta_1\gamma_h\theta_v\mu_v^2\rho_h^2c_1^2 \\
&+ a^2L_v^2\alpha_h\beta_1^2\gamma_h\theta_v\rho_h^3c_1^2 + 4ab_1d_1\alpha_h\beta_1\theta_v\mu_v^2\rho_h^2c_1^3 + 2ab_1^2d_1\alpha_h\beta_1\theta_v\mu_v^2\rho_hc_1^3
\end{aligned}$$

$$\begin{aligned}
A_2 &= 3a_1b_1^3d_1^2\alpha_h\theta_v\mu_v^2c_1^3 + a^2Ka_1b_1d_1L_v\beta_1\beta_2\mu_v^2\rho_h^2c_1^3 + a^2a_1b_1\alpha_h\beta_1^2\theta_v\mu_v^2\rho_h^2c_1^3 \\
&+ 3a_1b_1d_1^2\alpha_h\theta_v\mu_v^2\rho_h^2c_1^3 + 4aa_1b_1d_1\alpha_h\beta_1\theta_v\mu_v^2\rho_h^2c_1^3 + a^2a_1b_1L_v^2\alpha_h\beta_1^2\theta_v\rho_h^2c_1^3 \\
&- a^3Ka_1b_1L_v^2\beta_1^2\beta_2\theta_v\rho_h^2c_1^3 + a^3Ka_1b_1d_1L_v\beta_1^2\beta_2\mu_v\rho_h^2c_1^3 \\
&+ 2a^2a_1b_1L_v\alpha_h\beta_1^2\theta_v\mu_v\rho_h^2c_1^3 + 4aa_1b_1d_1L_v\alpha_h\beta_1\theta_v\mu_v\rho_h^2c_1^3 \\
&- a^3Ka_1b_1L_v\beta_1^2\beta_2\theta_v\mu_v\rho_h^2c_1^3 - a^2Ka_1b_1d_1L_v\beta_1\beta_2\theta_v\mu_v\rho_h^2c_1^3 \\
&+ a^2Ka_1b_1^2d_1L_v\beta_1\beta_2\mu_v^2\rho_hc_1^3 + 6a_1b_1^2d_1^2\alpha_h\theta_v\mu_v^2\rho_hc_1^3 \\
&+ 4aa_1b_1^2d_1\alpha_h\beta_1\theta_v\mu_v^2\rho_hc_1^3 + 4aa_1b_1^2d_1L_v\alpha_h\beta_1\theta_v\mu_v\rho_hc_1^3 \\
&- a^2Ka_1b_1^2d_1L_v\beta_1\beta_2\theta_v\mu_v\rho_hc_1^3 - a^2Kqd_1L_v\beta_1\beta_2\gamma_h\mu_v^2\rho_h^3c_1^2 \\
&+ a^3KqL_v^2\beta_1^2\beta_2\gamma_h\theta_v\rho_h^3c_1^2 - a^3Kqd_1L_v\beta_1^2\beta_2\gamma_h\mu_v\rho_h^3c_1^2 \\
&+ a^3KqL_v\beta_1^2\beta_2\gamma_h\theta_v\mu_v\rho_h^3c_1^2 + a^2Kqd_1L_v\beta_1\beta_2\gamma_h\theta_v\mu_v\rho_h^3c_1^2 \\
&- a^2Kqb_1d_1L_v\beta_1\beta_2\gamma_h\mu_v^2\rho_h^2c_1^2 + a^2Ka_1b_1d_1L_v\beta_1\beta_2\gamma_h\mu_v^2\rho_h^2c_1^2 \\
&+ 6a_1b_1d_1^2\alpha_h\gamma_h\theta_v\mu_v^2\rho_h^2c_1^2 + 4aa_1b_1d_1\alpha_h\beta_1\gamma_h\theta_v\mu_v^2\rho_h^2c_1^2 \\
&+ 4aa_1b_1d_1L_v\alpha_h\beta_1\gamma_h\theta_v\mu_v\rho_h^2c_1^2 - a^2Ka_1b_1d_1L_v\beta_1\beta_2\gamma_h\theta_v\mu_v\rho_h^2c_1^2 \\
&+ 6a_1b_1^2d_1^2\alpha_h\gamma_h\theta_v\mu_v^2\rho_hc_1^2 - a^2Kqd_1L_v\beta_1\beta_2\gamma_h^2\mu_v^2\rho_h^3c_1 \\
&+ a^2Kqd_1L_v\beta_1\beta_2\gamma_h^2\theta_v\mu_v\rho_h^3c_1 + 3a_1b_1d_1^2\alpha_h\gamma_h^2\theta_v\mu_v^2\rho_h^2c_1
\end{aligned}$$

$$\begin{aligned}
A_1 &= a^3a_1b_1\beta_1^2\beta_2c_1^3d_1K\mu_h\rho_h^2L_v\mu_v - a^3a_1b_1\beta_1^2\beta_2c_1^3K\mu_h\rho_h^2L_v^2\theta_v \\
&- a^3a_1b_1\beta_1^2\beta_2c_1^3K\mu_h\rho_h^2L_v\theta_v\mu_v + a^2a_1b_1\beta_1\beta_2c_1^2d_1Kq\gamma_h\rho_h^2L_v\theta_v\mu_v \\
&- a^2a_1b_1\beta_1\beta_2c_1^2d_1Kq\gamma_h\rho_h^2L_v\mu_v^2 - a^2a_1b_1\beta_1\beta_2c_1^2d_1K\gamma_h\mu_h\rho_h^2L_v\theta_v\mu_v \\
&+ a^2a_1b_1\beta_1\beta_2c_1^2d_1K\gamma_h\mu_h\rho_h^2L_v\mu_v^2 - a^2a_1b_1\beta_1\beta_2c_1^3d_1K\mu_h\rho_h^2L_v\theta_v\mu_v \\
&- a^2a_1^2b_1^2\beta_1\beta_2c_1^3d_1K\rho_hL_v\theta_v\mu_v - a^2a_1b_1^2\beta_1\beta_2c_1^3d_1K\mu_h\rho_hL_v\theta_v\mu_v \\
&+ a^2a_1b_1\beta_1\beta_2c_1^3d_1K\mu_h\rho_h^2L_v\mu_v^2 + a^2a_1^2b_1^2\beta_1\beta_2c_1^3d_1K\rho_hL_v\mu_v^2 \\
&+ a^2a_1b_1^2\beta_1\beta_2c_1^3d_1K\mu_h\rho_hL_v\mu_v^2 + 2aa_1^2b_1^2\beta_1c_1^3d_1\alpha_h\rho_hL_v\theta_v\mu_v \\
&+ 2aa_1^2b_1^2\beta_1c_1^3d_1\alpha_h\rho_h\theta_v\mu_v^2 + 3a_1^2b_1^2c_1^2d_1^2\alpha_h\gamma_h\rho_h\theta_v\mu_v^2 \\
&+ 3a_1^2b_1^2c_1^3d_1^2\alpha_h\rho_h\theta_v\mu_v^2 + 3a_1^2b_1^3c_1^3d_1^2\alpha_h\theta_v\mu_v^2
\end{aligned}$$

$$A_0 = a_1^3 b_1^3 c_1^3 d_1^2 \alpha_h \theta_v \mu_v^2 - a^2 a_1^2 b_1^2 \beta_1 \beta_2 c_1^3 d_1 K \mu_h \rho_h L_v \mu_v \alpha_v$$
$$= a_1^3 b_1^3 c_1^3 d_1^2 \alpha_h \theta_v \mu_v^2 \left(1 - R_O^2\right)$$

E. Climate Related Parameters

We assume that the mosquito birth rate depends on temperature and rainfall, given by the following formula [23]

$$\theta_v(T,R) = \frac{N_E S_E(R) S_L(R,T) S_P(R)}{\chi_E + \chi_L(T) + \chi_P}$$

where

- N_E represents the total number of Eggs laid per adult female mosquito.
- $S_E(R), S_L(R,T)$ and $S_P(R)$ are the survival probability of Eggs, Larvae and pupa, respectively.
- $\chi_E, \chi_L(T), \chi_P$, the duration of each aquatic stage.

Temperature and rainfall independently influence larvae's survival probability [23]. This leads to the equation $S_L(R,T) = S_{L1}(T) S_{L2}(R)$, where $S_{L1}(T)$ and $S_{L2}(R)$ represent the survival probability of larvae depending on temperature and rainfall respectively. Specifically, $S_{L1}(T)$ is given by $\mathrm{e}^{-\alpha T + \beta}$.

Rainfall has two side effects: it may either raise the frequency of malaria by providing adequate habitat for mosquitoes or decrease the prevalence by flushing away mosquito breeding sites. The survival probabilities of Eggs(E), Larvae(L) and Pupae(P) assume a quadratic relationship between them and rainfall defined as

$$S_i(R) = \left(\frac{4P_i^*}{R_w^2}\right) R(R_w - R) \quad \text{with } i = E, P, L \tag{24}$$

P_i^* represent the maximum survival probability of Eggs, Larvae, and Pupa and R_w is the wash-out limit for Eggs, Larvae and Pupae (= 50 mm).

The larvae duration varies with temperature and may be represented as [46]:

$$\chi_L(T) = \frac{1}{\alpha T + \beta} \quad \text{with } \alpha \text{ and } \beta \text{ constants} \tag{25}$$

The mortality rate of Mosquitoes is a temperature-dependent rate with function given by the following [23]:

$$\mu_v(T) = \frac{1}{AT^2 + BT + C} \tag{26}$$

where A, B, C are constants.

$L_v(T)$ which is the proportion of exposed mosquitoes that become infected is related to the ambient temperature

$$L_v(T) = \mathrm{e}^{-\mu_v(T)\left[\frac{DD}{T - T_{\min}}\right]} \tag{27}$$

where DD and $T_{\min}$ are the total degree days and the minimum temperature required for parasite development respectively, and $\left[\frac{DD}{T - T_{\min}}\right]$ is defined as the duration of the sporogonic cycle in days. This function suggests that the proportion

of mosquitoes that become infected is influenced by the ambient temperature, with higher temperatures generally promoting faster parasite development and shorter sporogonic cycles [47] [48].

The frequency with which the vectors take a blood meal each day determines the mosquito biting rate [42]

$$a(T) = A_1 T(T - A_2)\sqrt{A_3 - T} \tag{28}$$

and the frequency of feeding depends on how the blood meal is digested. It has been shown that as the temperature increases, the biting rate increases [23].